RESEARCH ARTICLE OPEN ACCESS

RELATIVE HUMIDITY MAPPING AND ITS APPLICATIONTO THE ANALYSIS OF PRESTRESSED LOSSES FOR PRESTRESSED CONCRETE BRIDGES IN THE PHILIPPINES

Carl John M. Aguilus[1], Erika Joni B. Carreon[2], Jeahnelle C. Malit[3], Brizzalyn V. Manalili[4], Paulo Aldrin L. Mendoza[5], Kris Dale V. Miguel[6], Raven M. Pangilinan[7], John Robert D. Gabriel[8], Reggie R. Martin[9]

[1]Department of Civil Engineering, Don HonorioVentura State University, Bacolor, Pampanga
Email:carljohn.m.aguilus@gmail.com
[2] Department of Civil Engineering, Don HonorioVentura State University, Bacolor, Pampanga
Email:carreonerikajoni@gmail.com
[3] Department of Civil Engineering, Don HonorioVentura State University, Bacolor, Pampanga
Email:jeahnellemalit@gmail.com
[4]Department of Civil Engineering, Don HonorioVentura State University, Bacolor, Pampanga
Email:brizzalynmanalili@gmail.com
[5]Department of Civil Engineering, Don HonorioVentura State University, Bacolor, Pampanga
Email:pauloaldrinmendoza@gmail.com
[6]Department of Civil Engineering, Don HonorioVentura State University, Bacolor, Pampanga
Email:dalemiguel0@gmail.com
[7]Department of Civil Engineering, Don HonorioVentura State University, Bacolor, Pampanga
Email:rav3n.m.pangilinan@gmail.com
[8]Department of Civil Engineering, Don HonorioVentura State University, Bacolor, Pampanga
Email: jrdgabriel@dhvsu.edu.ph
[6]Department of Civil Engineering, Don HonorioVentura State University, Bacolor, Pampanga
Email: rrmartin@dhvsu.edu.ph

----------**********----------

Abstract:

Aside from wind and seismic factors that can affect the bridges' serviceability, performance, and durability, relative humidity also needs to carefully be considered in designing of bridges. The influence of environmental relative humidity on concrete is mainly reflected in the movement of water in concrete and has a certain influence on the properties of concrete (such as drying shrinkage and creep). In this study, the researchers proposed a relative humidity map using a Quantum Geographic Information System (QGIS) that will be useful in the analysis of prestress loss to ensure the durability, safety, and economical reasons of the prestressed concrete bridges in the Philippines. This study will help to better understand the effect of relative humidity in prestressed concrete bridges. After conducting the study, the research findings are the following, the proposed map using QGIS software gives an accurate calculation of the long-term loss of the prestressed concrete, and the use of Weibull Formula and Microsoft Excel gives ease to determine the return levels presented in this study.

Keywords **—Relative HumidityMapping, Geographic Information System (GIS),Prestressed Concrete (PSC), Concrete Creep, Concrete Shrinkage, Approximate Method, Long-term or Time-dependent Losses**

----------**********----------

I. INTRODUCTION

The Pacific typhoon belt, a belt of active volcanoes, significant earthquake faults, and the western edge of the Pacific Ring of Fire all encircle the Philippines. With the longest continuous coastline in the world, measuring 32,400 km (about 20132.43 mi), it is particularly susceptible to the negative effects of climate change. It is one of the

world's most natural disaster-prone countries due to the high incidence of typhoons, floods, landslides, droughts, volcanoes, and earthquakes, and the country's considerable vulnerability to these hazards [1].

The Philippines experiences high temperatures and heavy amounts of rainfall due to its humid tropical environment. Rainfall varies widely, with an average of 2,348 millimetres (mm) in southeast Mindanao and over 4,050 mm in central Luzon every year. At 27°C on average year-round, the temperatures are often high, especially in the plains and valleys. Due to warm, humid trade winds that blow through the archipelago, lush, vibrant vegetation, high sea surface temperatures, and an abundance of rainfall, the region has high humidity levels, averaging about 82% [2].

Relative humidity is strongly variable with temperature, and air pressure also plays a role. The higher the air temperature the higher the maximum capacity of air to uptake water vapor, because the air expands with temperature. Also, the amount of water vapor in the air is known as relative humidity. Measurements of vapor pressure are used to calculate the variable relative humidity (RH). The formula, rh = ea/esat, expresses the ratio between the actual amount of water vapor in the air (ea) and the maximum amount of water vapor that the air can absorb at a given temperature (esat) [3].The effect of environmental relative humidity on pre-stressed concrete is mostly reflected in the movement of water vapor in pre-stressed concrete and has a certain influence on the properties of concrete (such as drying shrinkage and creep) [4].

Prestressed concrete is defined as concrete with stresses incorporated into the member. Typically, wires or "tendons" are stretched and then blocked at the ends, resulting in compressive pressures across the entire cross-section of the component. The majority of prestressed concrete is manufactured in a factory [5].

The following are the advantages of prestressed concrete: (a) The section remains uncracked under service loads. (b) A high span-to-depth ratio. (c) Ideal for precast construction. (d) Pre-stressed concrete utilizes its cross-section more efficiently than reinforced concrete. (e) Prestressed concrete enables longer spans. (f) Pre-stressed concrete members are more resistant to shear strain. (g) When considering the same depth of concrete member, a pre-stressed concrete member is stiffer than a reinforced concrete member under working loads. (h) The combination of high-strength concrete and steel produces a reduced cross-section. Even while pre-stressing has benefits, numerous factors must be carefully examined. Prestressing requires specialized technology. Thus, it is less common than reinforced concrete. (a) Using high-strength materials is pricey. (a) There is an additional charge for auxiliary equipment. There is a requirement for quality control and inspections. (d) Prestressed concrete portions have lower fire resistance[6].

As pre-stressed concrete structures become more complex, interest in creep and shrinkage has grown. More vulnerable to its effects have emerged, as have structural damages or problems encountered (creep and shrinkage) [7]. Creep and shrinkage deformations are equivalent to elastic deformations in pre-stressed concrete structures. These deformations frequently produce severe cracking and deflections, as well as probable failure, resulting in a loss of serviceability, durability, and long-term safety of concrete structures [8] Drying shrinkage is the volume loss that concrete experiences because of moisture migration when exposed to a lower relative humidity environment than the initial one in its pore system. Creep is the time-dependent strain caused by the application of constant stress over time. Its dual mechanism is known as relaxation, and it is the time-dependent reduction of stress caused by a constant deformation level in time [9].

Relative humidity must be considered while designing prestressed concrete bridges for several reasons. The choice of the structural design parameters can be greatly influenced by relative humidity maps, which display the proportion of moisture in the air.

Relative humidity maps must be incorporated into the design of prestressed concrete bridges to maximize these vital infrastructure elements' structural performance, longevity, and viability from an economic standpoint. By guaranteeing that the structure can endure the local environmental

conditions, it lowers the need for maintenance and lengthens the bridge's lifespan.

In the Philippines, Bridge engineers do not have detailed and site-specific relative humidity data, which is critical for accurate assessments of material performance, corrosion rates, and long-term durability of bridge structures. This gap in environmental information can hinder the ability to make fully informed decisions regarding maintenance, design, and safety measures.

An accurate relative humidity map is crucial for the design of prestressed concrete bridges in the Philippines, a country known for its tropical climate and archipelagic geography. There are several interconnected reasons for this, including ensuring the bridges' structural integrity, longevity, durability, and service life, as well as their economic efficiency and sustainability.

Moreover, a Geographic Information System (GIS), also known as a geospatial information system, allows for the recording of a base map utilizing a geographic referencing system such as latitude and longitude. This technology then allows you to undertake geographical analysis by superimposing additional layers of discrete geographic information on top of the base map.GIS – is a special case of information systems where the database consists of observations on spatially distributed features, activities, or events, which are definable in space as points, lines, or areas. It manipulates data about these points, lines, and areas to retrieve data from ad hoc queries and analyses.

GIS software includes a variety of statistical and analytical techniques that can be used to investigate the correlations between different spatial information. This enables the user to visualize patterns and trends throughout a landscape [10].

1.2 REVIEW OF RELATED LITERATURE

1.2.1 Prestressed Concrete

High-strength prestressing steel (PS) tendons are used in post-tensioned concrete. Tensed after casting, these tendons pre-compress the concrete slab and provide exceptional control over structural deflections while the structure is in operation. In contrast to conventional (non-prestressed) reinforced concrete slabs, post-tensioned concrete uses high-strength cold-drawn prestressing steel (PS) tendons. These tendons, when tensioned inside ducts in the concrete after casting, compress the concrete slab and produce excellent control of in-service deflections. There are two types of post-tensioned concrete: bonded (where the PS tendon is grouted within a steel or plastic duct and is thereby continuously bonded to the concrete after tensioning) and unbonded (where the PS tendon is greased and sheathed within the concrete, preventing bond to the surrounding concrete). As a means of achieving strict ecological and aesthetic goals in modern, optimized buildings, post-tensioned concrete structures are becoming more and more common [11]. The capacity to create longer clear spans, which permits more open and flexible environments, is one of post-tensioning's main benefits. Post-tensioning also makes it possible to utilize thinner slabs, which lowers the building's overall height and the floors' overall height. This lessens the structure's weight in addition to producing a more aesthetically beautiful appearance. A further noteworthy benefit is the enhanced seismic performance, as post-tensioning aids in the uniform distribution of stresses during an earthquake. Finally, post-tensioning speeds up the construction cycle, resulting in time savings and increased building process efficiency [12].

Pre-tensioning is when the tendons made of high-strength steel are pulled between two end abutments (also known as bulkheads) before the concrete is cast. The support beams are anchored at the prestressing bed's ends [13]. Compared to post-tensioning, pre-tensioning has several benefits.

First, it is an affordable option for mass manufacturing since it works especially well for the large-scale manufacture of precast parts. Furthermore, huge, costly, and labor-intensive mooring systems are no longer necessary with pre-tensioning. This lowers the cost of personnel and materials while streamlining the construction process.

Pre-tensioning also gives you more control over the strength and quality of the concrete, which makes your constructions stronger and more dependable. All things considered, pre-tensioning is a very effective and affordable way to reinforce

precast elements. Pre-tensioning has certain benefits, but it also has certain drawbacks. The requirement for a pre-stressing bed, which raises the operation's overall cost and complexity, is one significant disadvantage. In addition, the pre-stressing bed has a waiting period since the concrete must have enough time to strengthen before it can be discharged. The necessity of a solid link between the concrete and steel throughout the transmission length is another important consideration. The pre-tensioned components' structural integrity may be jeopardized by any flaws in this relationship. Pre-tensioning projects need to be properly planned for and addressed to minimize these drawbacks [12].

Reinforced Concrete a combination of steel reinforcement with concrete to give the concrete the tensile strength it lacks is known as reinforced concrete. In addition to being utilized in columns, steel reinforcing may withstand compression forces in other contexts that will be covered in a later section [14]. Because of the following benefits, reinforced concrete has been utilized in many different applications, including buildings, bridges, roads, pavements, dams, retaining walls, tunnels, arches, domes, shells, tanks, pipes, chimneys, cooling towers, and poles. The following are the advantages of RC. (a) Molded to any shape. (b) Availability of materials. (c) Low maintenance. (d) Water and fire resistance. (e) Good rigidity. (f) Compressive strength. (g) Economical. (h) Low-skilled labor. The following are the disadvantages. (a) Low tensile strength. (b) Requires forms and shoring. (c) Relative low strength [15].

Pre-stressed concrete was created in the early 20th century and began to be used extensively by engineers around 1928. Furthermore, prestress is a technique that uses pre-compression to reduce stresses caused by external loads below the neutral axis of the beam but not to the point where they exceed the allowable limits of plain concrete. Pre-compression that is applied (which may be axial or eccentric) causes compressive stress to be created below the neutral axis or throughout the entire beam c/s. either no tension or compression as a result. To counterbalance the stresses brought on by the external loads to the necessary extent, pre-stressed concrete essentially entails the introduction of internal stresses of a suitable magnitude and distribution [16].

Figure. 1 Prestressed Concrete
Source:

A typical reinforced concrete structure differs from a prestressed concrete structure in that the initial was subjected to a load before use. The starting weight, or "prestress," is used to give the structure the ability to withstand the pressures that will occur over its service life. [6] The following are the advantages of prestressed concrete: (a) The section remains uncracked under service loads. (b) A high span-to-depth ratio. (c) Ideal for precast construction. (d) Pre-stressed concrete utilizes its cross-section more efficiently than reinforced concrete.(e) Prestressed concrete enables longer spans. (f) Pre-stressed concrete members are more resistant to shear strain. (g) When considering the same depth of concrete member, a pre-stressed concrete member is stiffer than a reinforced concrete member under working loads. (h) The combination of high-strength concrete and steel produces a reduced cross-section. Even while pre-stressing has benefits, numerous factors must be carefully examined. Prestressing requires specialized technology. As a result, prestressed and reinforced concrete are rarely used. (a) Using high-strength materials is pricey. (a) There is an additional charge for auxiliary equipment. There is a requirement for quality control and inspections. (d) Pre-stressed concrete portions have lower fire resistance [6].

1.2.2 Effect of Prestressed Losses in Prestressed Concrete

The decrease of initially imposed pre-stress to an effective value is referred to as pre-stress loss. This loss is of tremendous significance since it impacts a member's strength as well as its serviceability, including stresses in concrete, cracking, camber, and deflection. There are two types of prestress loss

which the short-term or immediate losses and the long- term or time-dependent losses.

Short-term or immediate lossesoccur during the pre-stressing of tendons and the transfer of pre-stress to the concrete member. These include the following:

Elastic Shortening

The abrupt compression of concrete that happens when a prestress load passes through the concrete's hardened part is what causes loss due to elastic shortening. Prestressing steel can shorten along with the concrete as it does so. It is described as the combination of the stress gained from the member's self-weight and the loss of tensile stress in prestressing steel. The average stress in the concrete at the prestressing steel level and the modular ratio determine the elastic shortening [17].

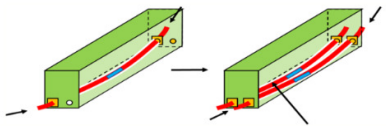

Figure. 2Elastic Shortening
Source:

Wobble Friction

Wobble friction is created by accidental contact with the distorted area of a duct, and it can cause the duct to wobble [18]. Even in a straight sheath, wobble friction can arise due to an unexpected distortion of the sheath that can occur during the handling or casting of concrete. This can happen even if the sheath is supported at a particular interval before casting takes place [19].

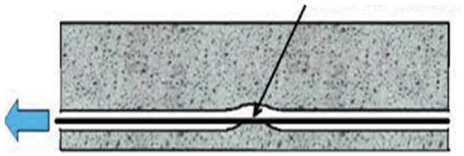

Figure. 3Wobble Friction
Source:

Long-term or Time-dependent Losses: These losses occur during the service life of the structure. These include the following:

Concrete Creep

Creep is the term used to describe the extended, time-dependent deformation of concrete under continuous compressive load or stress. There are two categories of concrete creep: basic creep and advanced creep, which is gradually drying out. Basic creep is the ongoing deformation that takes place in a sealed specimen exposed to an environment of hydro equilibrium. An exposed specimen goes through more creep, or drying creep, brought on by the environment's unrestricted moisture exchange. Prestress is lost because of the concrete girder's protracted shortening. The rate of creep is dependent on several variables, including time, stress level, water-cement proportion, kind and quantity of cement, surrounding relative humidity, and aggregate characteristics [17].

Figure. 4Concrete Creep
Source:

Concrete Shrinkage

The concrete specimen's volumetric contraction is brought on by the removal of free water. In the absence of a load, evaporation, carbonation, or continuous cement hydration are referred to as diminution. It is made up of three parts: carbonation, autogenous shrinkage, and drying shrinkage. Concrete's volume decreases because of water diffusion. It is known as the drying of the environment.When autogenous shrinkage happens, after hardening, free water is still used to continue hydrating the cement mix. Carbonation arises from the chemical reaction of carbon dioxide from the environment with a solidified cement mix. Once again, the carbonation process uses free water response. Regardless of the cause of the shrinkage, the concrete's volume reduction results in an overall strand length reduction, which lowers strand stress and leads to prestress damage [17].

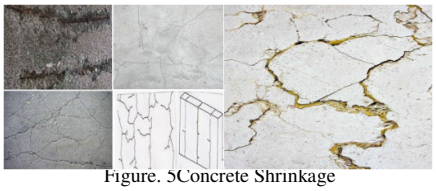

Figure. 5Concrete Shrinkage
Source:

Relaxation

The slow, steady lowering of tension brought on by prolonged strain is known as relaxation. It takes

place without the steel's length changing. Prestressing steel has a feature called relaxation, which is unrelated to the characteristics of the concrete. The most common types of low-relaxation prestressing strands typically have losses that do not exceed 5 ksi [17].

1.2.3 Effect of Relative Humidity in Prestressed Concrete

The effect of water/cement ratio, cement type, curing time, and exposure duration on time-dependent relative humidity profiles in drying concrete is investigated. The pre-stressed concrete's water/cement ratio and initial moist curing possessed little effect on the measured relative humidity for laboratory exposure, but the latter dropped faster in pre-stressed concrete made with pulverized fuel ash or ground granulated blast furnace slag than in those made with ordinary Portland cement. A series of simple equations was used to express the relative humidity in pre-stressed concrete subjected to laboratory exposure. High relative humidity levels were detected in pre-stressed concrete exposed to the elements, although these were reduced when the exposed area was protected from rain. The consequences of concrete performance are briefly discussed, as are the advantages of relative humidity measurements [20].

Relative humidity and temperature are different from other environmental parameters. Their impacts on items are more varied and complex than those of the other elements, and they are interrelated. For one object, an acceptable temperature or relative humidity may be disastrous. It is not possible to completely eradicate temperature and relative humidity; instead, appropriate values for each must be found. It is insufficient to just provide an average number for temperature and relative humidity because these variables also have an impact on objects. Temperature affects relative humidity, and temperature determines the feasible range in which it can be managed [21].

Concrete creep models with humidity factors have been developed and planned in foreign countries, including the Committee European Concrete Institute (CEB), American Concrete Institute (ACI) as well as Bazant.

These models' properties are related to the effect of humidity on concrete creep and drying concrete shrinkage so that the concrete shrinkage is used to generate a concrete creep prediction model amid humidity [4]. Furthermore, the creep and shrinkage of concrete are influenced by many factors including relative humidity and temperature. The combined effect of low relative humidity and high temperature on the creep and shrinkage of concrete is uncertain as limited tests have been conducted in this domain [17].

In addition, the concrete shrinkage is the result of the concrete gradually getting shorter over time; the tendon gets shorter, and the prestress force is reduced tendon relaxation is the gradual, progressive lowering of tendon stress. Both tendon temperature and length are constant. Concrete creep is when the concrete gradually gets shorter over time. The tendon shortens because of creep, lowering the prestress force [22].

1.2.4 Map used in Designing Prestressed Concrete Bridges in the Philippines

With an average of 20 tropical cyclones every year passing through the Philippine Area of Responsibility (PAR), nine of which make landfall, windstorms rank 1st as the worst natural disaster, which is known to be the most disaster-prone country of the 20th century. Although the impact of devastating earthquakes receives a lot of attention, it ranks as the Philippines' second-worst disaster [23].

Wind Map

Wind load is one of the structural actions which has a great deal of influence on bridge design. The significant role of wind loads is highlighted after it caused several bridge structures to collapse completely.

Wind can provide serious problems for bridge constructions, especially when it comes to strong gusts, persistently high winds, or unique wind patterns like those of tornadoes or hurricanes. The design of the bridge, the wind's direction and speed, and the building materials all affect the kinds of damage that the wind might do.

The nature of the wind load is dynamic. This means that its magnitude varies in terms of time and space. As a result, analysis and modeling of such a

load and its relative effects on the structure may be quite complex and require substantial knowledge in mathematics, computational fluid dynamics, and structural analysis [24].

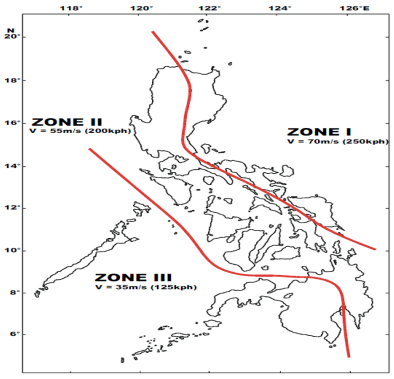

Figure. 6Wind Map of the Philippines
Source:

Seismic Map

Due to the geographical location of the Philippines and the numerous numbers of volcanoes, as a result, the country is highly vulnerable to volcanic eruptions and earthquakes. Because of their inherent susceptibility, seismic maps are essential for a variety of planning, development, and safety objectives.

Significant earthquake damage can cause bridge structures to collapse fully or partially. The magnitude and depth of the earthquake, distance from the epicenter, bridge design and construction quality, and surrounding geology can all influence the extent and type of damage.

Maps with seismic attributes have grown in importance as instruments for the structural analysis of seismic data. The feature maps have been shown to be particularly useful in locating small structures, such as faults beneath or near seismic resolution. Bridge design must take seismic maps into account, particularly in earthquake-prone areas. The likelihood, frequency, and intensity of possible seismic activity are all determined by the data found on seismic maps [25].

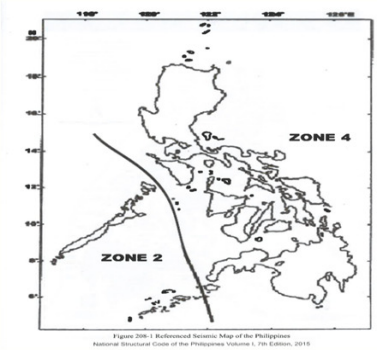

Figure. 7Seismic Map of the Philippines
Source:

Relative Humidity Map

In the Philippines, the need for a detailed relative humidity map is crucial for several reasons, especially when it comes to infrastructure development like the design and maintenance of prestressed concrete (PSC) bridges to assure the constructability and serviceability of the bridge, the prestress loss is used in design to estimate the stress in the concrete at various sections (mostly to prevent cracking in the concrete) and to estimate deformations of the beam [26].

Thus, the researchers propose a relative humidity map that shows the relative humidity percentage of each station in the Philippines which will be useful in designing bridge

1.2.5 Geographic Information System (GIS)

The term 'GIS software' often refers to software for creating, managing, analysing, and visualizing geographic data. GIS software is commonly used for evaluating locations for new stores, managing power and gas lines, creating maps, analysing past crimes for crime prevention, calculating routes for transportation tasks, managing forests, parks, and infrastructure, such as roads and waterways, and risk analysis of natural hazards and emergency planning and response [27].

Quantum Geographic Information System - QGIS

QGIS is an open-source Geographic Information System. QGIS aims to provide a user-friendly GIS with common functionality and features. The project's initial purpose was to develop a GIS data viewer. QGIS has evolved to the point where it is used for everyday GIS data viewing, data capture,

advanced GIS analysis, complex maps, atlas, and report presentations. QGIS supports a wide range of raster and vector data formats, with additional format compatibility easily added via the plugin architecture [28].

ArcGIS

The Environmental Systems Research Institute, or Esri, is the company behind ArcGIS, a comprehensive geographic information system (GIS) software. It is used to create, manage, analyse, and map numerous forms of geographical data. It is employed in the creation, administration, analysis, and mapping of various types of geographic data. Using globes, maps, reports, and charts, ArcGIS enables users to comprehend, display, and interpret data to identify links, patterns, and trends. ArcGIS provides a scalable framework for implementing GIS for a single user or many users on desktops, on servers, over the web, and in the field. ArcGIS is an integrated suite of advanced GIS applications [29].

Surfer

Surfer is a grid-based mapping tool that transforms irregularly spaced XYZ data into a consistently spaced grid. Grids are also accessible from other organizations, such as the United States Geological Survey (USGS). The grid is used to create various types of maps, including contour, vector, image, shaded relief, watershed, 3D surfaces, and 3D wireframe. A range of gridding and mapping options are available, allowing you to design the map that best represents your data [30].

1.2.6 Relative Humidity Mapping Attempt

Mapping relative humidity, average and extreme temperature in hot summer over China

Air temperature and relative humidity are the key variables in environmental health research. Both are difficult to map, especially on a national scale because of spatial heterogeneity. This paper presents a methodology for mapping relative humidity, average, and extreme temperatures in hot summer (June to August) over China. Several data as explanatory variables were applied to random forest regression models to predict relative humidity and temperatures, including surface reflectance, land cover, digital elevation model (DEM), enhanced vegetation index (EVI), latitude, night-time lights (NLs), as well as buffer zones of road, railroad, river system, and administration centre. Results based on cross-validation reflect acceptable prediction errors in estimating relative humidity (RMSE = 7.4%), average temperature (RMSE = 2.4 °C), average maximum temperature (RMSE = 2.5 °C), and extreme maximum temperature (RMSE = 2.6 °C). Despite the strong correlation between average and extreme temperatures, significant differences exist in their spatial distribution along the latitude direction, especially in areas such as Hebei, Szechwan, Hubei, Henan, Shandong, and Inner Mongolia. Specifically, socioeconomic activity, relative humidity, and vegetation tend to affect extreme heat events, and both latitude and DEM (i.e., geographical position) determine the average level of temperature. Compared with interpolation technology and statistical methods, the proposed methodology demonstrates the ability to generate relative humidity and temperature maps with finer gradients in hot summer over China [31].

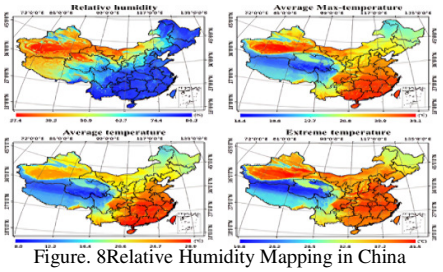

Figure. 8Relative Humidity Mapping in China

Source:

Climatology and Trends of U.S. Surface Humidity and Temperature

Surface-specific humidity (q) and relative humidity (U) regulate evaporation and transpiration processes and so have obvious connections to both hydrological and surface energy budgets. However, despite current interest in quantifying and modeling these budgets, there is a lack of observational datasets describing the recent surface climatology of humidity over the United States. The two main purposes of this paper are to present climatological, seasonal surface humidity distributions over the United States for the recent climatic normal period 1961–90 and to evaluate trends in several humidity variables and temperatures over the period 1961–95. The source of data for this study is the National

Solar Radiation Data Base (NSRDB; NREL 1992; which includes hourly meteorological and solar radiation data for 239 stations in the (50) United States and territories for 1961–90 and updated through 1995 (T. Ross, National Climatic Data Center, 1997, personal communication). These are surface airways observations from the NWS first-order stations. We employ the hourly pressure (p), T, and U data and compute Td, q, vapor pressure (e), and Ta. For Ta, we ignore the effects of wind and radiation and employ Steadman's (1984) regression equation. Ta=-1.3+0.92T+2.2e, where T is Celsius, and e is kPa. Beyond the NSRDB quality control (NREL 1992), we rejected all interpolated data and observations that were not physically reasonable.

Data were accepted within the following ranges: for temperature and dewpoint, 2708 to 608C (with the provision that Td # T); for relative humidity, 0%–100%; and for pressure, 600– 1100 hPa. From 1965 to 1981 meteorological data were saved only for every third hour, namely, 0300, 0600, 0900, ..., and 2400 UTC, which led to somewhat different sampling of the diurnal cycle in different time zones. However, this diminished sampling has negligible impact on climatological monthly means. RIJC found that climatological monthly dewpoint values based on 24 and 8 observations per day differ by less than 0.18C, based on more than 10 yr. of data for which 24 hourly observations were available at 222 stations [32].

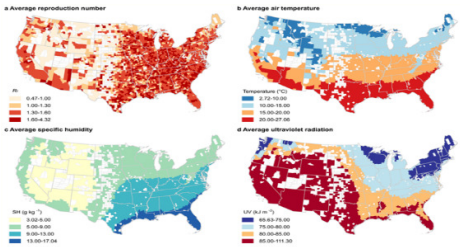

Figure. 9Relative Humidity Mapping in United States
Source:

1.2.7 AASHTO LRFD Bridge Design Specifications for Prestress Loss

Load Transfer

$$\Delta f_{pR} = \frac{\log(24t)}{40}\left(\frac{f_{pj}}{f_{py}} - 0.55\right) f_{pj} \quad 5.9.5.4.4b-2$$

Where:

t = time in days from stressing to transfer

f_{pj} = initial stress in the tendon after anchorage seating

f_{py} = specified yield strength of prestressing steel

Long Term Losses - Approximate Method

$$\Delta f_{pLT} = 10\frac{f_{pi}A_{ps}}{A_g}\gamma_h\gamma_{st} + 12\gamma_h\gamma_{st} + \Delta f_{pR}$$

Where:

f_{pi} = prestressing steel stress immediately prior to transfer (ksi)

H = the average annual ambient relative humidity (%)

γ_h = correction factor for relative humidity of ambient air

= 1.7-0.01H

γ_{st} = correction factor for specified concrete strength time at of prestress transfer

to concrete member

= 5/(1+ f'_{ci})

ΔfpR = Estimate of relaxation loss taken as 17 MPa for low relaxation strand, 70 MPa for stress relieved strand, in accordance with manufacturers recommendation for other types of strands (MPa).

Concrete shrinkage before deck placement

$$\Delta f_{pSR} = \varepsilon_{bid}E_pK_{id}$$

Where:

ε_{bid} = shrinkage strain of girder concrete between time of transfer or end of curing and time of deck placement

K_{id} = transformed section coefficient that accounts for time-dependent interaction between concrete and bonded steel in section being considered for period between transfer and deck placement.

Concrete creep before deck placement

$$\Delta f_{pCR} = \frac{E_p}{E_c}f_{cgp}\psi_b(t_d, t_i)K_{id}$$

Where:

E_{ci} = modulus of elasticity of concrete at transfer

f_{cgp} = concrete stress at centroid of prestressing tendons due to the prestressing force immediately

after transfer and self-weight of the member at section of maximum moment
$\psi_b(t_d, t_i)$= creep coefficient for girder concrete at the time td of deck placement due to loading applied at the time at transfer t_i

Girder concrete shrinkage after deck placement

$$\Delta f_{psD} = \varepsilon_{hdf} E_p K_{df}$$

Where:
ε_{hdf} = shrinkage strain of girder concrete after deck placement
K_{df} = transformed section coefficient that accounts for time-dependent interaction between concrete and bonded steel in section being considered after deck placement

Concrete creep after deck placement

$$\Delta f_{pDD} = \frac{E_p}{E_d} f_{css}[\psi_s(t_f, t_i) - \psi_s(t_d, t_f)]K_* + \frac{E_p}{E_c}\Delta f_{\alpha d}[\psi_s(t_f, t_d)]K_d$$

Where:
$\psi_s(t_f, t_i)$ = creep coefficient for girder concrete at final time t_f due to loading applied at the time t_i of transfer
$\Delta f_{\alpha d}$= change in concrete stress at centroid of prestressing strands due to time-dependent loss of prestress between transfer and deck placement combined with deck weight and superimposed loads
$\psi_s(t_f, t_d)$ = creep coefficient for girder concrete at final time t_f due to loading applied at time t_d of deck placement

1.3 STATEMENT OF THE PROBLEM

Prestressed concrete bridge infrastructures are essential in making ways to connect two points between rivers, islands, and regions in the Philippines. However, the environmental conditions in the country, including high temperatures and varying humidity levels, pose significant challenges to the long-term durability of these structures. The Relative Humidity (RH) within the concrete elements is a critical factor that affects the performance and service life of prestressed concrete bridges.:

a. How can we use the relative humidity data from PAGASA in developing a relative humidity map using Quantum Geographic Information System (QGIS) software, what is the possible appearance of the map and where is the maximum relative humidity percentage located in the Philippines?
b. How to determine the 10, 20, 30, 40, and 50-year-return period of relative humidity percentage of each station in the Philippines?
c. How to apply the relative humidity map in the analysis of prestress losses of a prestressed concrete bridge?

1.4 OBJECTIVES

1.4.1 General Objective

This study aims to create a Relative Humidity Map and its useful application in to the analysis of prestressed losses of the Prestressed Concrete Bridges in the Philippines.

1.4.2 Specific Objective

Specifically, the research study aimed to:
a. To create a relative humidity map using Quantum Geographic Information System (QGIS) Software.
b. To determine the 10,20,30,40 and 50-year return period of relative humidity percentage of each station in the Philippines by relative humidity modeling using Weibull Formula and Microsoft Excel.
c. To apply the Relative Humidity (RH) map in the analysis of prestress losses of prestressed concrete bridges in the Philippines.

SCOPE AND LIMITATIONS

The study aims to create an accurate and detailed relative humidity map of the Philippines. This map will help to understand the spatial variations of relative humidity, which can be crucial for various applications.

Additionally, it is important to acknowledge the limitations of the study specifically historical data possibly affecting the completion of the analysis.

Thus, these limitations will be carefully considered in the course of the study to ensure an accurate interpretation of the dynamics of relative humidity in the abovementioned scope.

II. METHODOLOGY

2.1 Research Design

This study is conducted through the use of descriptive research, a design approach that focuses on Relative Humidity Mapping and its Application to Pre-stressed Concrete Bridges in the Philippines.

As defined by Winston Salem State University (n.d), Descriptive Research aims to describe an identified variable on its status. This type of research is designed to provide information on a certain phenomenon in a systematic way. In a usual circumstance, the researchers do not begin with a hypothesis, but they usually develop one after data has been collected.

Additionally, data, including Relative Humidity Mapping from PAGASA, and plans of the Prestressed Concrete Bridge from DPWH, will be gathered for quantitative analysis

Moreover, the development of Relative Humidity Mapping will be analyzed through the QGIS Software while the Application of the Plan of Prestressed Concrete Bridge from DPWH will be examined through manual calculation of prestressed losses [34].

2.2 Methodological Framework

The research study is divided into three phases: Data Analysis, Development of Relative Humidity Map using Quantum Geographic Information System (QGIS) Software, Application of Relative Humidity (RH) Map by reanalyzing Pre-stressed Concrete (PSC) Bridges from Department of Public Works and Highways (DPWH).

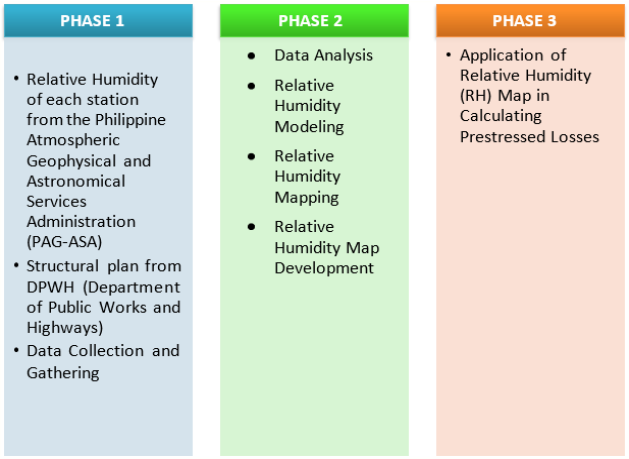

2.3 Data Analysis

In this study, the researcher will consider the data received from the Philippine Atmospheric, Geophysical, and Astronomical Services Administration (PAGASA) to improve the study's accuracy. PAGASA is the government agency in charge of delivering timely, accurate, and dependable weather forecasts and other meteorological information to the public and other sectors in the Philippines. Using their data, researchers may gain a better understanding of the region's weather patterns and conditions, which is crucial for their analysis.
As a result, the researcher will examine this data using several statistical and analytical tools before making meaningful recommendations. These will enable the researcher to make more informed conclusions and recommendations based on the findings of the investigation.

2.4 Relative Humidity Modelling

The second phase of the study is relative humidity modeling. The gathered relative humidity data of each PAGASA weather station was built to a Weibull distribution. These were done using Microsoft Excel. The 50-year return period of relative humidity data was established.

Weibull Formula

$$P = \frac{m}{N+1}$$

Where:

P = Probability of exceedance

N =Number of years of record

m = Rank

$$T = \frac{1}{P}$$

Where:

P = Probability of exceedence

T = Return Period

2.5 Relative Humidity Mapping

The third phase includes software to make the relative humidity map. The researchers seek help from the expert on which mapping software is suitable for their research. Experts suggest different kinds of mapping software like ArcGIS, QGIS, and SURFER. The researchers considered the availability and functionality of the software to be used. ArcGIS and Surfer are commonly used in making a contour map, but it is expensive software while QGIS is a free, open-source software that allows users to create, edit, visualize, analyse, and publish geospatial information. For that reason, the researcher came up with the use of QGIS in developing the relative humidity map.

2.5.1 Relative Humidity Map Development

The 50-year return period of Relative Humidity values taken from the gathered annual RH data were used to represent Z-values of the data while X and Y values were taken from coordinates on the data given from PAGASA (coordinates of synoptic weather stations). These processed data were used as input to find the appropriate gridding method to be used and do an objective analysis (computer-generated output). Gridding methods were used to produce regularly spaced rectangular arrays of Z values from XYZ data. The XYZ data are normally irregularly spaced and follow no pattern over the map. This produced many gaps where the gridding fills by interpolating or extrapolating values at locations where there is no available data.

There are several methods for gridding and each method may look like the other when plotted or different depending on the application of the map being produced for the given XYZ values. A Quantum Geographic Information System (QGIS) was used for the evaluation and selection of the gridding methods.

The following are the gridding methods in QGIS

1. Inverse Distance Weighted
2. Kernel Density Estimation
3. Modified Quadratic Shephard
4. Natural Neighbour
5. Nearest Neighbour
6. Shapes to Grid
7. Triangulation

The selection of the appropriate gridding method was narrowed to only one.

1. Inverse Distance Weighted (IDW) Interpolation Method - the sample points are weighted during interpolation such that the influence of one point relative to another declines with distance from the unknown point you want to create.

2.6 Application of Relative Humidity (RH) map by reanalyzing the prestressed concrete bridges

Using the proposed relative humidity value based on the relative humidity map as a parameter for the long-term loss of prestress concrete. Calculate the long-term loss using AASHTO specification as guidelines with the method of approximation and refined method.

2.6.1 Total Loss of Prestress

Reference Formulas (AASHTO) for long-term losses where relative humidity is a function of creep and shrinkage effects:

In pretensioned members (total loss of prestress)

$$\Delta \boldsymbol{fPT} = \Delta fPES + \Delta fPLT$$

In post tensioned members (total prestress)

$\Delta \boldsymbol{fPT} = \Delta fPF + \Delta fPA + \Delta fPES + \Delta fPLT$

Where:

$\Delta \boldsymbol{fPT}$ = Total loss (MPa)

$\Delta \boldsymbol{fPF}$ = Loss due to friction (MPa)

$\Delta \boldsymbol{fPA}$ = Loss due to anchorage set (MPa)

$\Delta \boldsymbol{fPES}$ = Sum of losses or gains due to elastic shortening or extension at the time of application of prestress and / or external loads (MPa)

$\Delta \boldsymbol{fPLT}$ = Losses due to long term shrinkage and creep of concrete, and relaxation of steel (MPa)

2.6.2 Approximate Estimate of Time-Dependent Losses

2.6.2.1 Long term prestress loss

$$\Delta \boldsymbol{f_{PLT}} = 10\frac{f_{pi}Aps}{Ag}\gamma_h\gamma_{st} + 83\gamma_h\gamma_{st} + \Delta_{f\,pr}$$

$$\boldsymbol{\gamma h} = 1.7 - .01$$

$$\boldsymbol{\gamma_{st}} = \frac{35}{(7 + f_{ci})}$$

Where:

$\Delta \boldsymbol{f_{PLT}}$ = long term -prestress loss

$\boldsymbol{f_{pi}}$ = prestressing steel immediately prior to transfer (MPa)

$\boldsymbol{Aps}$= Area of prestressing steel (mm^2)

$\boldsymbol{Ag}$ = Gross area of section (mm^2)

$\boldsymbol{\gamma_h}$ = Correction factor for relative humidity of ambient air

H = Average annual ambient relative humidity (%)

$\boldsymbol{\gamma_{st}}$ = Correction factor for specified concrete strength at time of prestress transfer to concrete member

$\boldsymbol{f_{ci}}$= Specified compressive strength of concrete at time of initial loading or prestressing (MPa)

$\Delta_{f\,pr}$= Estimate of relaxation loss taken as 17 MPa for low relaxation strand, 70 MPa for stress relieved strand, in accordance with manufacturers recommendation for other types of strands (MPa).

III. RESULTS AND DISCUSSIONS

3.1 Results and Discussions

This chapter presents the study's findings by the methods provided in the previous chapter. To examine the data, the researchers employ tables. The data collected from PAGASA's fifty-nine (59) stations were tallied. Certain yearly relative humidity values from numerous stations were missing for a variety of reasons, and the station no longer ran concurrently beginning in 1994.

The return period of the relative humidity percentage at each station was determined using the annual relative humidity data from PAGASA. The 10, 20, 30, 40, & 50-year return period is displayed in Table 3.1. The relative humidity contour map was proposed using the Inverse Distance Weighted approach for gridding method selection. The researchers consider using a 50-year return period in proportion to the lifespan of the bridge.

The developed relative humidity contour map was produced using the 50-year return level of relative humidity value. Using the contouring method in QGIS. Figure 3.3 shows the relative humidity map of the Philippines with the actual percentage in 50-year reoccurrence. The minimum value of the contour line is 81%, while the maximum value of the contour line is 102%. In the proposed map, it was observed that the relative humidity percentage in the northeast of the Philippines was higher than in the other parts of the Philippines. The observed relative humidity percentage of each province was determined by considering the nearest contour line in the province.

Table3.110,20,30,40 & 50 Year Return Period Relative Humidity Percentage**.**

NO.	STATION	10 years	20 years	30 years	40 years	50 years
1	Alabat	85.96	87.16	87.87	88.37	88.76
2	Ambulong	85.77	87.60	88.67	89.43	90.02
3	Aparri	85.27	85.93	86.32	86.60	86.61
4	Baguio	90.78	92.15	92.96	93.53	93.97
5	Baler Radar	87.89	89.11	89.83	90.34	90.74
6	Basco Radar	90.01	93.09	94.89	96.17	97.16

7	Borongan	89.66	90.70	91.30	91.73	92.07
8	Butuan	86.65	88.01	88.81	89.38	89.82
9	Cabanatuan	88.88	91.42	92.90	93.96	94.78
10	Calapan	86.28	87.09	87.56	87.89	88.15
11	Calayan	88.76	90.33	91.25	91.96	92.41
12	Casiguran	90.49	91.93	92.77	93.37	93.83
13	Catarman	88.6	90.0	90.9	91.5	91.9
14	Catbalogan	84.97	86.45	87.32	87.93	88.41
15	Clark	78.84	80.78	81.91	82.71	83.33
16	Coron	87.19	89.72	91.20	92.25	93.07
17	Cotabato	78.69	79.82	80.48	80.95	81.32
18	Cubic Point	76.25	77.66	78.49	79.08	79.53
19	Cuyo	86.95	88.33	89.14	89.71	90.15
20	Daet	95.05	98.16	99.97	101.26	102.26
21	Dagupan	86.13	87.73	88.67	89.33	89.85
22	Dauis	86.40	87.51	88.17	88.63	88.99
23	Davao City	83.93	85.65	86.65	87.36	87.91
24	Dipolog	88.36	90.22	91.31	92.08	92.68
25	Dumaguete	83.85	85.12	85.86	86.38	86.79
26	El Salvador	88.66	88.66	89.83	90.66	91.30
27	General Santos	82.41	84.25	85.32	86.09	86.68
28	Guiuan	89.44	90.22	90.69	91.01	91.27
29	Hinatuan	87.35	88.40	89.01	89.45	89.79
30	Iba	83.74	85.33	86.26	86.92	87.44
31	Iloilo	85.20	87.15	88.290	89.09	89.72
32	Infanta	88.39	89.60	90.32	90.82	91.21
33	Itbayat	89.13	90.62	91.50	92.12	92.60
34	Juban	88.25	89.36	90.01	90.47	90.83
35	Laoag	81.27	82.48	83.19	83.69	84.09
36	Legazpi	86.60	87.76	88.43	88.91	89.28
37	Lumbia	86.04	87.50	88.35	88.95	89.42
38	Maasin	88.31	90.77	92.20	93.22	94.02
39	Mactan	87.09	89.92	91.58	92.75	93.66
40	Malaybalay	88.23	89.72	90.60	91.22	91.731
41	Masbate	85.31	86.50	87.19	87.68	88.06
42	NAIA	81.51	84.08	85.58	86.64	87.47
43	Port Area	77.36	78.82	79.68	80.29	80.76
44	Puerto Princesa	84.88	86.86	88.02	88.84	89.430
45	Romblon	84.30	85.51	86.22	86.72	87.11
46	Roxas City	84.09	85.06	85.63	86.04	86.35
47	San Jose	83.82	86.11	87.45	88.40	89.13
48	Sangley Point	82.44	84.16	85.17	85.88	86.43
49	Science Garden	82.39	84.82	86.24	87.25	88.03
50	Sinait	81.07	82.21	82.87	83.34	83.70
51	Surigao	85.70	86.87	87.56	88.05	88.43
52	Tacloban	86.79	87.80	88.40	88.82	89.15
53	Tagbilaran	84.67	85.75	86.39	86.83	87.18
54	Tanay	91.50	92.77	93.51	94.04	94.45
55	Tayabas	87.07	88.12	88.74	89.18	89.52
56	Tuguegarao	81.41	83.43	84.61	85.45	86.10
57	Vigan	80.71	81.74	82.34	82.76	83.10
58	Virac Synop	90.69	92.62	93.75	94.56	95.18
59	Zamboanga	83.67	85.07	85.88	86.46	86.91

Table 3.1 shows the results obtained using Microsoft Excel and the Weibull formula, the results of 10,20,30,40, and 50-year return periods of relative humidity percentage of each station are presented in Table 3.1 of this study. After obtaining the return period of each station, the researchers concluded that from the 10, 20, 30, 40, and 50 return periods, station Daet (Camarines Norte) obtained the highest relative humidity percentage while the lowest is in station Cubic Pt. (Olongapo City, Zambales).

Table 3.2 Summary of data statistics obtained from RH values for Luzon.
Period observation 1994-2023

NO.	STATION	50-YEAR RETURN PERIOD
1.	Alabat, Quezon	88.76
2.	Ambulong, Batangas	90.02
3.	Aparri, Cagayan	86.81
4.	Baguio City, Benguet	93.97
5.	Baler Radar, Aurora	90.74
6.	Basco Radar, Batanes	97.16
9.	Cabanatuan, Nueva Ecija	94.78
10.	Calapan, Oriental Mindoro	88.15
11.	Calayan, Cagayan	92.41
12.	Casiguran, Aurora	93.83
15.	Clark Intl. Airport Pampanga	83.34
16.	Coron, Palawan	93.07
18.	Cubic Pt. Olongapo City, Zambales	79.54
19.	Cuyo, Palawan	90.16
20.	Daet, Camarines Norte	102.27
21.	Dagupan City, Pangasinan	89.85
26.	El Salvador, Misamis	91.31

	Oriental	
30.	Iba, Zambales	87.44
32.	Infanta, Quezon	91.22
33.	Itbayat, Batanes	92.61
34.	Juban, Sorsogon	90.83
35.	Laoag City, Ilocos Norte	84.09
36.	Legazpi City, Albay	89.29
41.	Masbate, Masbate	88.07
42.	NAIA, Pasay City	87.47
43.	Port Area, Manila	80.76
44.	Puerto Princesa, Palawan	89.49
45.	Romblon, Romblon	87.11
47.	San Jose, Occidental Mindoro	89.14
48.	Sangley Point, Cavite	86.44
49.	Science Garden, Quezon City	88.03
50.	Sinait, Ilocos Sur	83.7
54.	Tanay, Rizal	94.45
55.	Tayabas, Quezon City	89.53
56.	Tuguegarao, Cagayan	86.1
57.	Vigan City, Ilocos Sur	83.1
58.	Virac Synop, Catanduanes	95.19

Table 3.2 presents the summary of obtained relative humidity values for Luzon. The values of relative humidity used are 50-year return period, by the lifespan of the bridges. After obtaining the 50-year return period of each station, the researchers concluded that, station Daet (Camarines Norte) obtained the highest relative humidity percentage while the lowest is in station Cubic Pt. (Olongapo City, Zambales).

Table 3.3 Summary of data statistics obtained from RH values for Visayas.
Period observation 1994-2023

No.	Station	50-year return period
7.	Borongan, Eastern Samar	92.07
13.	Catarman, Northern Samar	92.48
14.	Catbalogan, Western Samar	88.41
22.	Dauis, Bohol	88.99
25.	Dumaguete City, Negros Oriental	86.79
31.	Iloilo City, Iloilo	89.73
28.	Guiuan, Eastern Samar	91.27
38.	Maasin, Southern Leyte	94.02
39.	Mactan Intl. Airport, Cebu	93.66
46.	Roxas City, Aklan	86.35
52.	Tacloban City, Leyte	89.16
53.	Tagbilaran City, Bohol	87.19

Table 3.3 portrays the summary of obtained relative humidity values for Visayas. The values of relative humidity used are 50-year return period, by the lifespan of the bridges. After obtaining the 50-year return period of each station, the researchers concluded that station Maasin (Southern Leyte) obtained the highest relative humidity percentage while the lowest is in station Roxas, City (Aklan).

Table 3.4 Summary of data statistics obtained from RH values for Mindanao.
Period observation 1994-2023

No.	Station	50-year return period
8.	Butuan City, Agusan Del Norte	89.82
17.	Cotobato City, Maguindanao	81.32
23.	Davao City, Davao Del Sur	87.91
24.	Dipolog, Zamboanga Del Norte	92.68
27.	General Santos, South Cotobato	86.68
29.	Hinatuan, Surigao Del Sur	89.79
37.	Lumbia, Cagayan de Oro	89.43
40.	Malaybalay, Bukidnon	91.71
51.	Surigao, Surigao Del Norte	88.43
59.	Zamboanga City, Zamboanga Del Sur	86.92

Table 3.4 displays the summary of obtained relative humidity values for Mindanao. The values of relative humidity used are 50-year return period, by the lifespan of the bridges. After obtaining the 50-year return period of each station, the researchers concluded that station Dipolog (Zamboanga Del Norte) obtained the highest relative humidity percentage while the lowest is in station Cotabato, City (Maguindanao).

3.2 Relative Humidity Map Development

The following are steps in developing the Relative Humidity map using QGIS.

Step 1: Tabulate all the data for Latitude, Longitude and Relative Humidity Values with 50-year return period using Microsoft Excel.

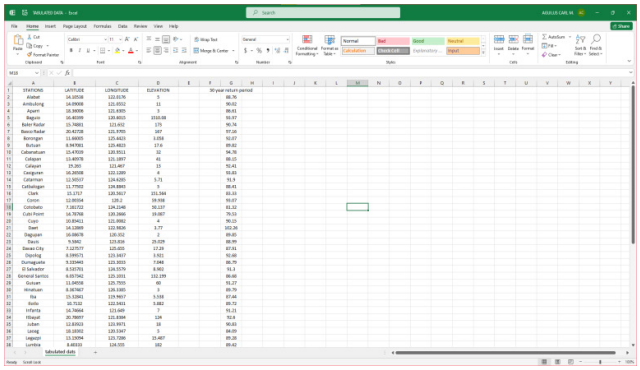

Step 2: Open QGIS 3.32

Step 3: Save the tabulated data as CSV. File first, then add it as delimited text in QGIS 3.32

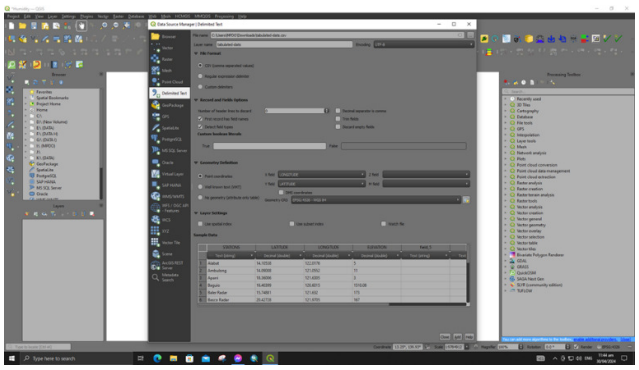

Step 4: Save as shapefile layer the tabulated data and boundary

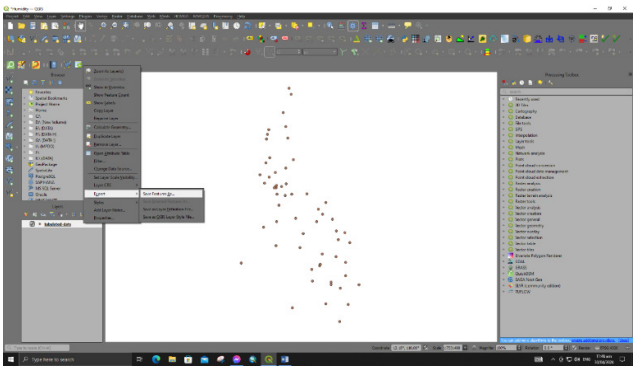

Step 5: Type IDW in tool box then select IDW interpolation method

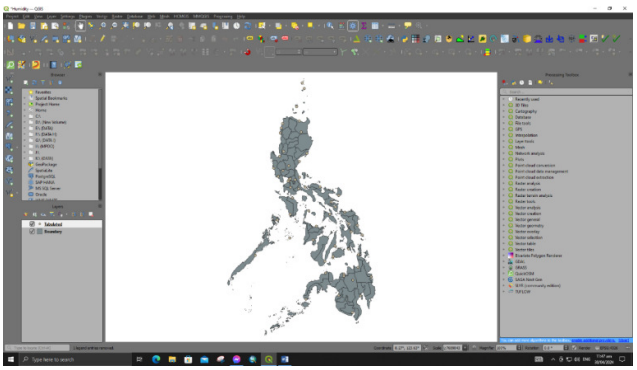

Step 6: In the IDW tab, follow set up and save as interpolated then click run.

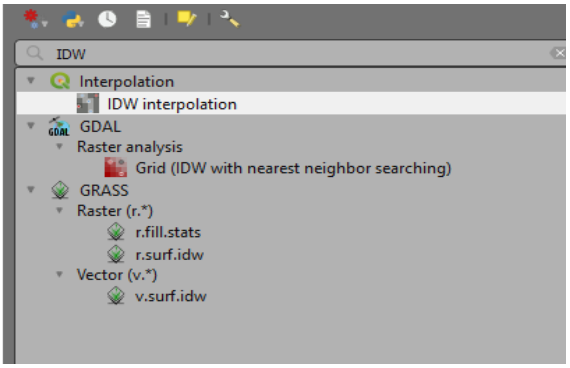

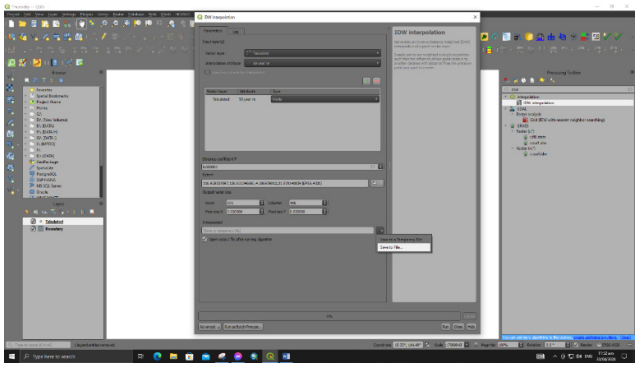

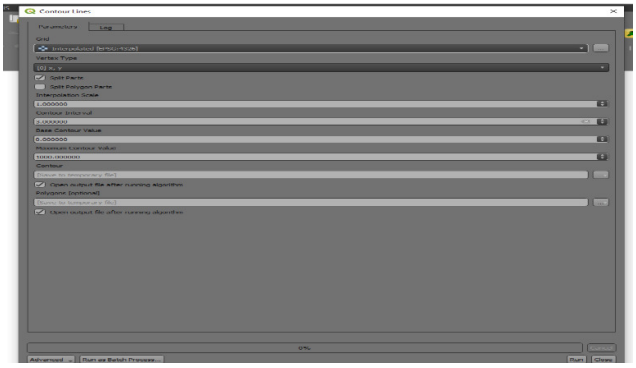

Step 7: Follow the symbology set up for the data visualization

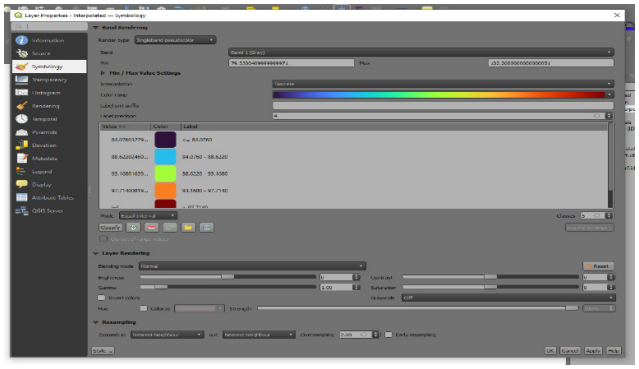

Step 8: Type in the toolbox the contour tool and select it.

Step 10: Click Layer Properties- contour-labels. Set up for contour label

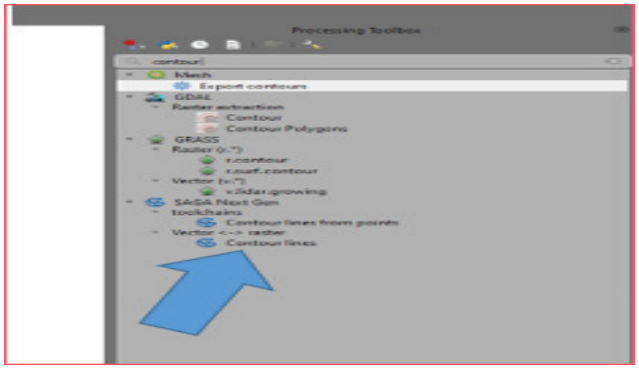

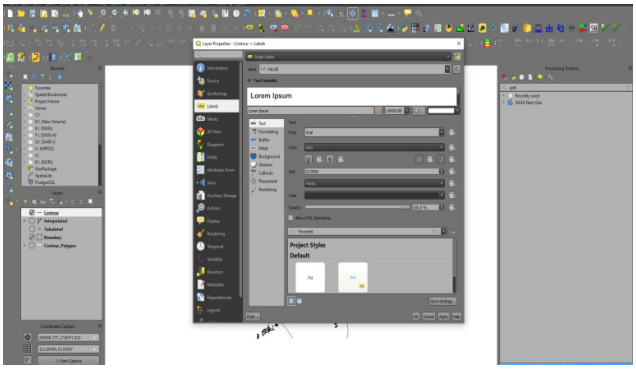

Step 9: In the contour tab just follow the setup then click run.

Step 11: Set up for text placement

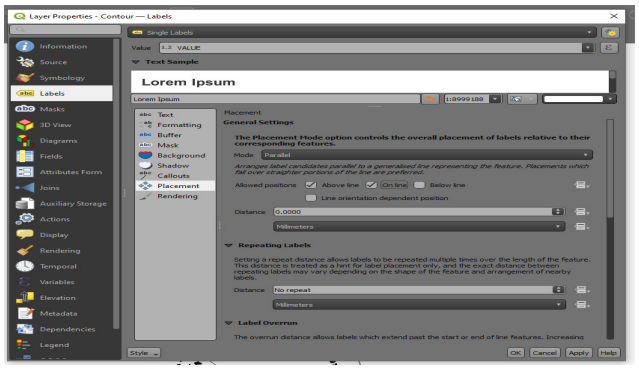

Output without colour of **Step 11**

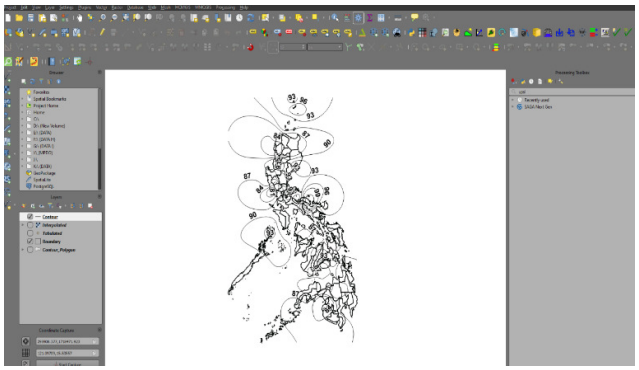

Output with colour of **Step 11**

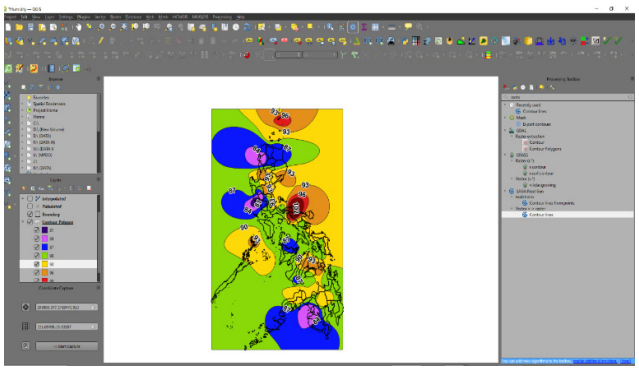

The following shows the Inverse Distance Weighted (IDW) Interpolation Method with and without the fill contours. Interval (3)

With Colour

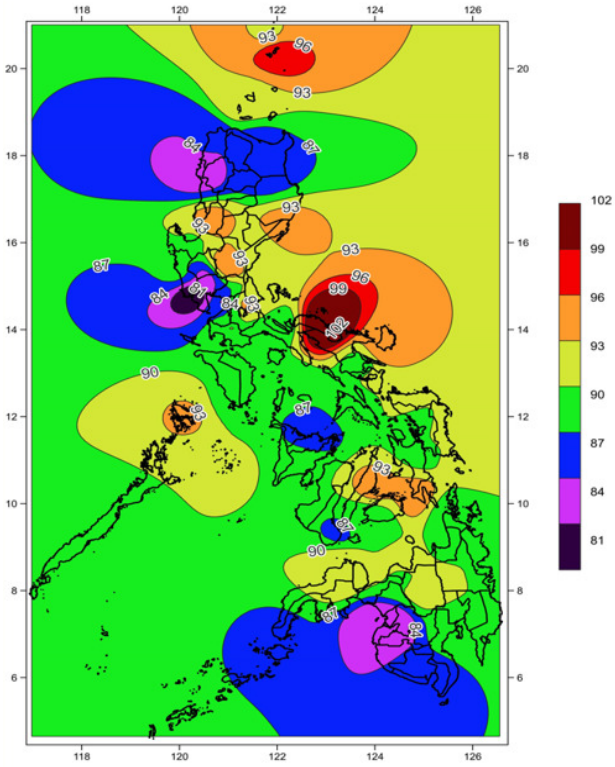

Figure. 21Inverse Distance Weighted (IDW) Interpolation Method
Source:

Without Color

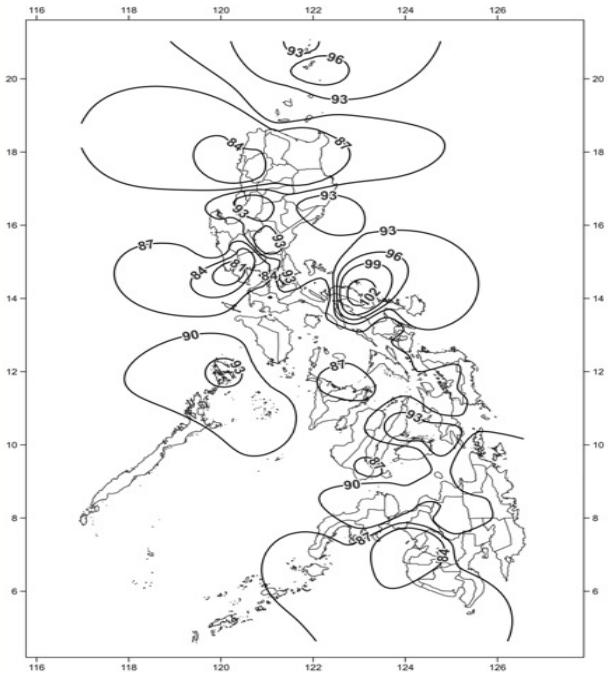

Figure. 22Inverse Distance Weighted (IDW) Interpolation Method

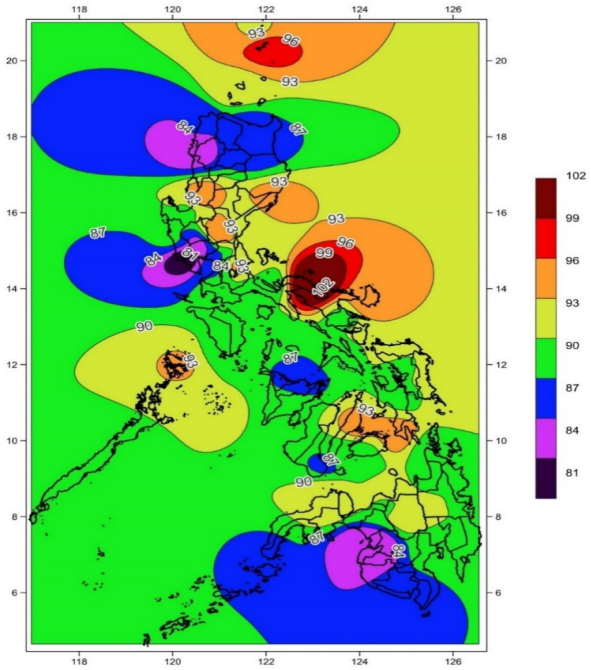

Figure. 23Propose Relative Humidity Map
Source:

Figure 23 shows the proposed relative humidity map, wherein it depicts the levels of relative humidity in the Philippines using colour and its corresponding percentage.

Table 3.5 Relative humidity Value With 50-year Return Period

Relative Humidity (%)	Provinces
80%	Cubic Pt. Olongapo City, Zambales.
82%	Port Area, Manila. Cotobato City, Maguindanao.
83%	Clark Intl. Airport Pampanga. Vigan City, Ilocos Sur.
84%	Laoag City, Ilocos Norte. Sinait, Ilocos Sur.
86%	Sangley Point, Cavite. Tuguegarao, Cagayan. Roxas City, Aklan.
87%	Aparri, Cagayan. Iba, Zambales. NAIA, Pasay City. Romblon, Romblon. Dumaguete City, Negros Oriental. Tagbilaran City, Bohol. General Santos, South Cotobato. Zamboanga City, Zamboanga Del Sur.
88%	Masbate, Masbate. Science Garden, Quezon City. Catbalogan, Western Samar. Davao City, Davao Del Sur. Surigao, Surigao Del Norte.
89%	Alabat, Quezon. Legazpi City, Albay. Puerto Princesa, Palawan. San Jose, Occidental Mindoro. Dauis, Bohol. Tacloban City, Leyte. Lumbia, Cagayan de Oro.
90%	Ambulong, Batangas. Butuan City, Agusan Del Norte. Cuyo, Palawan. Dagupan City, Pangasinan. Tayabas, Quezon City. Iloilo City, Iloilo. Butuan City, Agusan Del Norte. Hinatuan, Surigao Del Sur.
91%	Baler Radar, Aurora. El Salvador, Misamis Oriental. Infanta, Quezon. Juban, Sorsogon. Guiuan, Eastern Samar.
92%	Borongan, Eastern Samar. Calayan, Cagayan. Catarman, Northern Samar. Malaybalay, Bukidnon.
93%	Coron, Palawan. Itbayat, Batanes. Dipolog, Zamboanga Del Norte.
94%	Baguio City, Benguet. Casiguran, Aurora. Tanay, Rizal. Maasin, Southern Leyte. Mactan Intl. Airport, Cebu.
95%	Cabanatuan, Nueva Ecija. Virac Synop, Catanduanes.
97%	Basco Radar, Batanes.
102%	Daet, Camarines Norte.

Based on the assessment of the researchers in Table 3.5, the relative humidity percentage with a 50-year return period in the Philippines is relatively high ranging from 80% to 102%. The major reasons for high humidity are the Philippines is in a warm current (temperature), the rainy season covers about half of the year, and the seasonal monsoon contains moist air and blows the Philippines all year long.

3.3 Calculation of Long-term Loss in Prestressed Concrete Bridge using Approximate Method.
AASHTO Type-IV

The bridge has a span length of 30.00 m. (c/c pier distance) and a total width of 9.54 m. The bridge superstructure consists of 4 AASHTO Type-IV B beam spaced at 2.30 m. center to center designed to act compositely with 200.0 mm. thick cast in place concrete deck. The wearing surface thickness is 50 mm. HL-93 is the design live load. The bridge will be constructed in Aurora. Use Approximate method to determine long-term prestress loss.

NOTATIONS:

A_g = gross area of precast section (mm2)

A_{ps} = area of prestressing steel (mm2)

$f`_{ci}$= specified compressive strength of concrete at time of prestressing for pretensioned members and at time of initial loading for non-PSC members. If concrete age at time of initial loading is unknown at design time f'ci may be taken as 0.80f'c (MPa)

f_{pi} = prestressing steel stress immediately prior to transfer (MPa)

H = relative humidity

Δf_{pLT} = losses due to long-term shrinkage and creep of concrete, and relaxation of the steel (MPa)

Δf_{pR}= Estimate of relaxation loss taken as 17MPa for low relaxation strand, 70MPa for stress relieved strand, in accordance with manufacturers recommendation for other types of strands (MPa).

y_h = correction factor for relative humidity of ambient air.

y_{st} = correction factor for specified concrete strength at time of prestress transfer to the concrete members

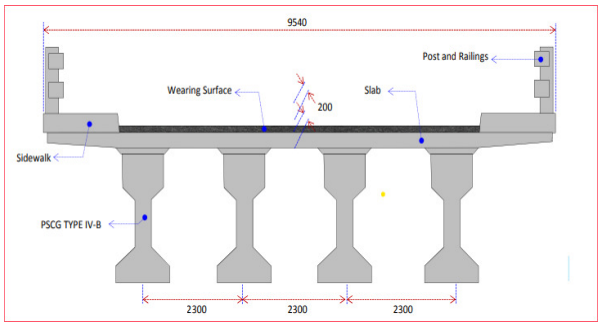

DESIGN PARAMETERS:

Pre-cast beams:

AASHTO Type-IV	
A_g = 611900 mm^2	*Gross area of concrete section*
$f`_{ci}$ = 27.6 *MPa*	*Concrete strength at release*
$f`_c$ = 28 *MPa*	*Concrete strength at 28 days*
γ_{cb} = 23.6 *MPa*	*Unit weight of concrete*

Pre-stress strands: (12.7mm diameter, seven wire low relaxation)

AASHTO Type-IV	
A_p = 98.71mm^2	*Area of one strand*
f_{pu} = 1860 *MPa*	*Ultimate strength of prestressing strand*
f_{py} = 1675.8 *MPa*	*Yield strength*
f_{pi} = 1253.93 *MPa*	*Stress of prestressing strand before transfer*
f_{pe} = 1343.61 *MPa*	*Stress of prestressing strand at service*
E_p = 197,000 *MPa*	*Modulus of Elasticity*
N_s = 36 *pcs*	*No. of strands*

3.3.1 Relative Humidity Values

The average annual ambient relative humidity is based from assume.

H = 91% - Aurora

3.3.2 Correction Factorfor Specified Concreteat Timeat Prestress Transferto the Concrete

$$\gamma_{st} = \frac{35}{7 + f_{ci}}$$

$$\gamma_{st} = \frac{35}{7 + (27.6)}$$

$$\gamma_{st} = 1.01$$

3.3.3 Correction Factor for Relative Humidity of Ambient Air

$$\gamma_h = 1.7 - 0.01H$$

$$\gamma_h = 1.7 - 0.01(91)$$

$$\gamma_h = 0.79$$

3.3.4 Long-term Losses

$$PLT = 10.0\frac{f_{pi}A_{ps}}{A_g}\gamma_h\gamma_{st} + 83\gamma_h\gamma_{st} + \Delta f_{pR}$$

$\Delta f_{pR} = 17$ MPa for low relaxation strand

$$PLT = 10.0\frac{(1253.93)(36)(98.70)}{(611900)}(1.01)(0.79) + 83(1.01)(0.79) + (17)$$

$$\boldsymbol{PLT = \underline{141.52MPa}}$$

The following are the researchers concluded:

- From the comparison of sample computation, the researchers concluded that the value of long-term losses decreased from 158.85MPa to 141.52MPa.

- The relative humidity value is inversely proportional to the long-term losses. When the value of relative humidity is low, the long-term loss value is high and when the value of humidity is high the value of long-term losses is low.

- Using the actual relative humidity value in calculating long-term losses can identify the appropriate design needed that can resist the losses that can affect the prestressed concrete during its lifespan

IV. SUMMARY, CONCLUSIONS AND RECOMMENDATIONS

4.1 Summary of Findings

Relative humidity continues to affect the country's infrastructure. To construct a pre-stressed concrete bridge, a relative humidity map of the Philippines was created through the study. Weibull Distribution was used to model relative humidity. QGIS was utilized for relative humidity mapping. Relative humidity was applied to bridges through computation utilizing a purely approximative approach. In general, high values were detected in the RH data collected nationwide. As a result, the estimated losses from shrinkage and creep were minimal. When utilizing the relative humidity contour map to compute pre-stress losses resulting from creep and shrinkage, the closest relative humidity value associated with the area where the structure is being constructed was chosen.

4.2 Conclusion

These are the following conclusions that have been made after conducting the research study:

- QGIS software, even freeware, is effective in making a contour map. The map's appearance contained the Philippines' geographical contour and gradient colors that show the variations in relative humidity across different areas. Higher humidity levels may be found in coastal locations, areas with dense vegetation, and places with large bodies of water compared to more arid or urban areas. After tabulating the return periods of each station together with their provinces which is shown in Table 3.5 of the study, due to its location which is near bodies of water and high temperature, the maximum relative humidity percentage is located at station Daet in the province of Camarines Norte.

- The usage of Weibull Distribution and Microsoft Excel gives expertise in determining the return level, which is illustrated in Table 3.1 of the study, and based on the return level of each station, relative humidity increased after 50 years.

- The developed map serves as a basis for finding the Relative Humidity (RH) percentage of an area for the calculation of the analysis of prestress losses of prestressed concrete bridges. The relationship of actual RH percentage to prestress loss is inversely proportional, as the RH increases the prestress loss decreases, and as the RH decreases the prestress loss increases.

4.3 Recommendations

In this study, the researchers used a Philippine map with regional boundaries, which is preferable over the previous zone maps because it reduces misinterpretation in using the map. For future studies, the researchers recommend the following:

- To use other software for making a contour map like ArcGIS.
- To use a spacing of four (4) unit intervals in presenting the relative humidity contour line for easy identification with each of the corresponding values plotted on the boundaries of the proposed map.
- To consider the relative humidity map in designing of vertical structure
- To possibly include of proposed relative humidity map in NSCP and DGCS 2015

REFERENCES

[1] M. Fernanda, G. Rincón, and F. K. Virtucio, "Country Environmental Analysis (CEA) Consultative Workshops held in Manila."
[2] "PHILIPPINES CLIMATE RISK COUNTRY PROFILE," 2021. [Online]. Available: www.worldbank.org
[3] "RELATIVE HUMIDITY & Climate Extremes." [Online]. Available: http://www.ghanalive.tv/2017/07/14/gawu-ghana-suffer-major-food-crisis-end-year/
[4] X. Dai, X. Zhang, L. Liu, and Y. Zou, "Influence of Environmental Humidity on Concrete Creep," in E3S Web of Conferences, EDP Sciences, Jan. 2019. doi: 10.1051/e3sconf/20197902005.
[5] "Lecture 24-Prestressed Concrete."
[6] M. Gude and R. Krishna, "LECTURE NOTES ON PRESTRESSED CONCRETE STRUCTURES Course code: A80150 Regulation: R15 (JNTUH) IV B. Tech II Sem PREPARED BY."
[7] Z. P. Ba~ant, "Theory of Creep and Shrinkage in 'Concrete Structures: A ·Precis of Recent Developments," Pergamon Press, Chapt. I.
[8] J. Karthikeyan and V. F. Praveen, "Long-term effects due to creep and shrinkage on prestressed concrete bridge girders using SCC," International Journal of Structural Engineering, vol. 2, no. 4, pp. 390–403, 2011, doi: 10.1504/IJSTRUCTE.2011.042902.
[9] "Chapter 3 DRYING SHRINKAGE AND CREEP IN CONCRETE: A SUMMARY."
[10] E. Ali, "Geographic Information System (GIS): Definition, Development, Applications & Components."
[11] J. Gales, L. Bisby, T. Stratford, and M. Krajcovic, "TESTS OF CONTINOUS POST-TENSIONED CONCRETE SLABS UNDER LOCALISED FIRES."
[12] V. Srilaxmi, K. Manju, and M. Vijaya, "A CASE STUDY ON PRE-TENSIONING & POST TENSIONING SYSTEMS OF A PRESTRESSED CONCRETE," International Journal of Engineering Technologies and Management Research, vol. 5, no. 2, pp. 249–254, Feb. 2020, doi: 10.29121/ijetmr. v5.i2.2018.169.
[13] A. K. Sengupta and P. Devdas Menon, "Prestressed Concrete Structures."
[14] "Design of Reinforced Concrete."
[15] S. Narayanan, "INTRODUCTION TO REINFORCED CONCRETE," 2013. [Online]. Available: http://en.wikipedia.org/wiki/Ingalls_Building
[16] J. Johnston, "Prestressed Concrete-Concept & Fabrication 2018 Bridge Construction Inspection School Learning Objectives 1. Define Prestressed Concrete 2. Member Types and Fabrication 3. Shop Drawings 4. Design Details 5. Things to Keep in Mind 2."
[17] H. Jayaseelan, G. R. Assistant, and B. W. Russell, "PRESTRESS LOSSES AND THE ESTIMATION OF LONG-TERM DEFLECTIONS AND CAMBER FOR PRESTRESSED CONCRETE BRIDGES FINAL REPORT," 2007.
[18] S. H. Kim, S. Y. Park, Y. H. Park, and S. J. Jeon, "Friction characteristics of post-tensioning tendons in full-scale structures," Eng Struct, vol. 183, pp. 389–397, Mar. 2019, doi: 10.1016/j.engstruct.2019.01.026.
[19] S.-J. Jeon, S.-Y. Park, S.-H. Kim, H.-K. Seo, S.-T. Kim, and Y.-H. Park, "MEASUREMENT OF FRICTION COEFFICIENT OF POST-TENSIONING SYSTEM USING SMART STRAND."
[20] L. J. Parrott, "Factors influencing relative humidity in concrete," 1991.
[21] D. Erhardt and M. Mecklenburg, "RELATIVE HUMIDITY RE-EXAMINED."
[22] S. West, "CivE 602 Prestressed Concrete Department of & Environmental Civil Engineering," 2011.
[23] "2005coetpu_philippines_report_Aquino".
[24] M. S. Mohammadi and R. Mukherjee, "Wind Loads on Bridges Analysis of a three span bridge based on theoretical methods and Eurocode 1," 2013.
[25] J. Hesthammer, "Evaluation of the timedip, correlation and coherence maps for structural interpretation of seismic data."
[26] "Prestress loss calculations - Another perspective".
[27] S. Steiniger and R. Weibel, "GIS Software-A description in 1000 words", doi: 10.5167/uzh-41354.
[28] "QGIS Desktop 3.16 User Guide QGIS Project," 2022.
[29] Esri, "What is ArcGIS?," 2001. [Online]. Available: www.esri.com,
[30] "Surfer ® 13 Powerful contouring, gridding & surface mapping system Full User's Guide." [Online]. Available: www.GoldenSoftware.com
[31] L. Li and Y. Zha, "Mapping relative humidity, average and extreme temperature in hot summer over China," Science of the Total Environment, vol. 615, pp. 875–881, Feb. 2018, doi: 10.1016/j.scitotenv.2017.10.022.
[32] D. J. Gaffen and R. J. Ross, "Climatology and trends of U.S. surface humidity and temperature," J Clim, vol. 12, no.

2–3, pp. 811–828, 1999, doi: 10.1175/1520-0442(1999)012<0811:catous>2.0.co;2.
[33] A. Gonzalez, M. Schorr, B. Valdez, and A. Mungaray, "Bridges: Structures and Materials, Ancient and Modern," in Infrastructure Management and Construction, IntechOpen, 2020. doi: 10.5772/intechopen.90718.
[34] "Key Elements of a Research Proposal - Quantitative Design."

